

Antenna Gain and Link Budget for Waves Carrying Orbital Angular Momentum (OAM)

Duy Kevin Nguyen¹, Olivier Pascal¹, Jérôme Sokoloff¹, Alexandre Chabory²,
Baptiste Palacin³, and Nicolas Capet³

¹LAPLACE, Laboratoire Plasma et Conversion d’Energie, Université de Toulouse UPS, F-31062 Toulouse, France,
e-mail: duy.nguyen@laplace.univ-tlse.fr,
olivier.pascal@laplace.univ-tlse.fr,
jerome.sokoloff@laplace.univ-tlse.fr.

²ENAC, TELECOM-EMA, F-31055 Toulouse, France, e-mail:
alexandre.chabory@recherche.enac.fr.

³CNES, Centre National d’Etudes Spatiales, antenna department, 18 avenue Edouard Belin, Toulouse, France, e-mail:
baptiste.palacin@cnes.fr,
nicolas.capet@cnes.fr.

This paper addresses the RF link budget of a communication system using unusual waves carrying an orbital angular momentum (OAM) in order to clearly analyse the fundamental changes for telecommunication applications. The study is based on a typical configuration using circular array antennas to transmit and receive OAM waves. For any value of the OAM mode order, an original asymptotic formulation of the link budget is proposed in which equivalent antenna gains and free-space losses appear. The formulations are then validated with the results of a commercial electromagnetic simulation software. By this way, we also show how our formula can help to design a system capable of superimposing several channels on the same bandwidth and the same polarisation, based on the orthogonality of the OAM. Additional losses due to the use of this degree of freedom are notably clearly calculated to quantify the benefit and drawback according to the case.

”This paper is a preprint of a paper submitted to AGU Radio Science and is subject to the American Geophysical Union Copyright. If accepted, the copy of record will be available at AGU Digital Library”

1. Introduction

From Maxwell’s theory, it is well-known that electromagnetic waves carry energy and both linear and angular momenta *Poynting* [1909]. The angular momentum has a spin component (SAM), associated with polarization, and an orbital component (OAM), related to the spatial distributions of the field magnitude and phase *Jackson* [1999]. The mechanical interaction between matter and these two components of the angular momentum has been theoretically and experimentally proven *Beth* [1936], *Niemiec et al.* [2012].

The SAM with two orthogonal states is well-known and widely exploited in operating systems to double the communication capacity. OAM has not yet been utilized in radio communications, even though it may represent a fundamental new degree of freedom *Djordjevic* [2011]. Indeed the use of OAM could help improving link capacities as controversially discussed in several recent papers *Tamburini et al.* [2012a], *Edfors and Johansson* [2012], *Tamagnone et al.* [2012] *Tamburini et al.* [2012b], *Tamagnone et al.* [2013], *Tamburini et al.* [2015].

From the 1990s, the OAM of light has been widely studied in optics with Laguerre-Gaussian beams *Allen et al.* [1992], *Padgett and Allen* [1995], *Gibson et al.* [2004], *Torres and Torner* [2011]. The results have been transposed to the radiofrequency

domain both theoretically *Thidé et al.* [2007], *Mohammadi et al.* [2010] and experimentally *Tamburini et al.* [2012a]. The generation of radio OAM waves can be performed in many ways, *e.g.* with a circular antenna array *Mohammadi et al.* [2010], a plane or spiral phase plate *Bennis et al.* [2013], *Beijersbergen et al.* [1994] or a helicoidal parabolic antenna with dedicated modifications *Tamburini et al.* [2012a], *Tamburini et al.* [2015]. The detection appears to be correctly achieved by an interferometer *Tamburini et al.* [2012a] or a 3D vector antenna *Diallo et al.* [2014]. Such configurations can also be analysed by means of classical communication tools for multiple-input-multiple-output (MIMO) antenna systems *Edfors and Johansson* [2012], *Tamagnone et al.* [2012].

In *Nguyen et al.* [2014], we have analysed the link between two antennas designed to transmit and receive OAM. We have found the same far-zone decay as previously exposed in *Tamagnone et al.* [2013]. We have also discussed the efficiency of OAM for radio communication. As in *Tamburini et al.* [2012a], *Edfors and Johansson* [2012], *Tamagnone et al.* [2012], *Thidé et al.* [2007] and *Bai et al.* [2014], a basic configuration using circular antenna arrays both to transmit and receive one single OAM mode has been studied and will be reused in the present paper. It exhibits the key advantage of a simple model through including the fundamental physical properties of OAM links.

The wave generated by the system is described by the modal orthogonality of the OAM associated with the rotating helical phase fronts. The antenna elements are fed with the same signal but at each element of the circular array, their phase vary

successively from 0 to $2\pi l$ circularly around the antenna array axis. The integer l is called the topological charge *Soskin et al.* [1997], where in quantum mechanics, $l\hbar$ is the OAM of one photon. The OAM topological charge l is not estimated as in *Mohammadi et al.* [2010], but the orthogonality property is exploited here for the possibility to superimpose several channels as it was experimentally performed in optics *Krenn et al.* [2014] and in RF *Tamburini et al.* [2012a].

In this paper, we propose to study the particular properties of the OAM link budget with respect to the OAM topological charge. The aim is to develop an asymptotic far-field formulation valid at large distances between two face-to-face circular array antennas. We use the equations of the link budget described in *Edfors and Johansson* [2012] and we add an asymptotic analysis that yields physical quantities that are suitable for a system design in a radio communication study with OAM.

The paper is organized as follows. In Section II, we summarize the theory of OAM link budget. In section III, an antenna array configuration is presented and studied first using the superposition principle. In section IV we find and validate an original asymptotic formulation of the link budget. In section V, for any value of the OAM order l , we define and study equivalent antenna gains and free-space losses. Finally, in section VI, the calculated formulations are validated using the results of the commercial electromagnetic simulation software Feko.

2. Theory

A link budget addresses the efficiency of a communication system. It takes into account for all the gains and losses from the transmitter to the receiver, associated with both antennas and the propagation channel.

In Fig. 1, D is the distance between the two antennas, P_t the transmitted power, G_t the transmitter antenna gain, P_r the received power, G_r the receiver antenna gain and L_{FS} the free-space losses. In its most concise form, P_r is given by the Friis transmission equation

$$P_r = \frac{P_t G_t G_r}{L_{FS}}. \quad (1)$$

In *Nguyen et al.* [2014], we have pointed out some difficulties in the calculation of the link budget. Indeed with classical considerations, no power can be received when the antennas are aligned for non-zero OAM orders due to the radiation patterns presented in *Mohammadi et al.* [2010] and depicted in Fig. 1. This asymptotic formulation questions the capability of OAM waves to support far-field communications.

3. Link budget for the two circular array configuration

In this section we introduce the equation of the transmission link as proposed by Edfors in *Edfors and Johansson* [2012]. In the next section, we go further by determining asymptotic equations that are more suitable for a system design in a radio communication study with OAM.

3.1. System configuration

In Fig. 2 we describe the configuration with which OAM modes of orders l are sent and OAM modes of orders l' are detected.

The transmission can be divided into three blocks: the Beam Forming Network (BFN) of the transmitter, the propagation channel, and the BFN of the receiver.

In Fig. 2, a_l^{OAM} and $b_{l'}^{\text{OAM}}$ are the complex input and output amplitudes of each transmitted or received mode, respectively. Furthermore, a_n^{feed} and b_p^{feed} are the wave amplitudes feeding the transmitter array or collected at the receiver array, respectively. The coefficient h_{pn} corresponds to the propagation term from the element n of the transmitter to the element p of the receiver.

A non-asymptotic configuration is considered in Fig. 3 as in *Edfors and Johansson* [2012] *Mohammadi et al.* [2010] with all the system parameters depicted. This system will be thoroughly described afterwards in this section. In *Nguyen et al.* [2014], the ratio of the received power of a mode of order l' and the transmitted power carried by a mode of order l has been explicitly formulated and numerically studied.

This article addresses how the link budget expression can be asymptotically expressed in a conventional form as in (1). For the sake of simplicity, we assume the following hypotheses:

1. Each array element is located using its phase center. The polarisation is the same for each antenna element, either linear or circular.
2. Mutual couplings are neglected.
3. Both BFNs are ideal.

Likewise, some considerations are assumed on the antenna parameters:

1. The number of antenna elements are the same for both arrays, $N = N_t = N_r$.

N is limited according to the sizes of the antenna array and the antenna elements.

2. The reference tilt angle between the two array antennas is zero, $\phi = 0$.

The configuration with two aligned circular array antennas facing each other is depicted in Fig. 3. In the following subsections, we study one by one the contribution of the blocks defined in Fig. 2.

3.2. BFN Matrix

On the one hand, to transmit several OAM modes of order l and amplitude a_l^{OAM} , the antenna elements must be fed by

$$a_n^{\text{feed}} = \frac{1}{\sqrt{N}} \sum_{l=0}^{N-1} a_l^{\text{OAM}} e^{-j2\pi \frac{ln}{N}}, n \in \{0, \dots, N-1\}, \quad (2)$$

with n the element index at the transmitter. This formulation defines an ideal BFN that has N input ports associated with the transmission of OAM modes of order $l \in \{0, \dots, N-1\}$. Note that the number of elements in the array limits the number of possible OAM modes due to sampling. Due to aliasing, modes of order greater than $N/2$ are actually modes of negative orders.

On the other hand, the BFN of the receiver builds at its output the OAM modes of order l' . The amplitude $b_{l'}^{\text{OAM}}$ must be so that

$$b_{l'}^{\text{OAM}} = \frac{1}{\sqrt{N}} \sum_{p=0}^{N-1} b_p^{\text{feed}} e^{j2\pi \frac{pl'}{N}}, p \in \{0, \dots, N-1\}, \quad (3)$$

with p the element index at the receiver.

From (2), the transmitter BFN matrix that relates the outputs a_n^{feed} to the inputs a_l^{OAM} is the matrix of the Discrete Fourier Transform (DFT) of size N , denoted \mathbf{U} . In the same way from (3), the receiver BFN matrix is the inverse discrete Fourier transform and can be characterized by the matrix \mathbf{U}^H .

3.3. Channel Matrix

The propagation channel of this system can be characterized by the channel matrix \mathbf{H} . Its terms h_{pn} correspond to the propagation from the phase center of the n -th element of the transmitter to the phase center of the p -th element of the receiver. The transfer function from the transmitter array and the receiver array is given by *Edfors and Johansson* [2012]

$$h_{pn} = \beta e^{-jkr_{np}} \frac{\lambda}{4\pi r_{np}}, \quad (4)$$

which gives the point-to-point link without coupling terms. The distance between each antenna element is given by

$$r_{np} = \sqrt{D^2 + R_t^2 + R_r^2 - 2R_t R_r \cos(\theta_{np})}, \quad (5)$$

with $\theta_{np} = 2\pi \left(\frac{n-p}{N}\right)$.

The free space losses are $4\pi r_{np}/\lambda$, the propagation term is the exponent, λ is the wavelength of the carrier.

β contains all the variables associated with the antenna system configuration. For the sake of simplicity, the two following hypotheses are added. Firstly, the elements of the transmitter and receiver antennas are in the far-field of each other. Secondly, for large distances between the two arrays, β is only related to their gains in the axial direction, therefore it can be approximated by $\sqrt{g_t g_r}$.

3.4. Single Mode Link Budget

Finally, the OAM link can be characterized by the matrix

$$\mathbf{H}_{\text{tot}} = \mathbf{U}^H \mathbf{H} \mathbf{U}. \quad (6)$$

This matrix gives all the relations, *e.g.* the crosstalk, between transmitted and received OAM modes. The output amplitudes are so that

$$\mathbf{b}^{\text{OAM}} = \mathbf{H}_{\text{tot}} \mathbf{a}^{\text{OAM}}. \quad (7)$$

By expanding the matrix products in (6) and (7), the ratio of the received and transmitted powers for only one OAM order l is given by

$$\frac{P_{\text{r}}}{P_{\text{t}}}(l) = \left| \frac{b_l^{\text{OAM}}}{a_l^{\text{OAM}}} \right|^2 = \left| \sum_{p=0}^{N-1} \sum_{n=0}^{N-1} \frac{\beta}{N} e^{-jl\theta_{np}} e^{-jkr_{np}} \frac{\lambda}{4\pi r_{np}} \right|^2. \quad (8)$$

This formulation can be expressed in a different way because the matrix \mathbf{H} is circulant. Indeed $h_{p,n}$ only depends on the difference $(n - p)$. From *Chan and Jin* [2007] the channel matrix is therefore diagonalized by the $N \times N$ unitary DFT matrix \mathbf{U} . Besides the eigenvalues κ_l of \mathbf{H} can be obtained from the DFT of the first row of \mathbf{H} .

This yields

$$\kappa_l = \sum_{n=0}^{N-1} h_{n,0} e^{-j\frac{2\pi ln}{N}}. \quad (9)$$

Finally, equation (6) is the diagonalisation of \mathbf{H} . This means that \mathbf{H}_{tot} is a diagonal matrix of elements κ_l and this shows the orthogonality of the OAM modes. The single-mode (*i.e.* $l = l'$) link budget can simply be expressed as

$$\frac{P_{\text{r}}}{P_{\text{t}}}(l) = |\kappa_l|^2 = \left| \frac{\lambda\beta}{4\pi} \sum_{n=0}^{N-1} \frac{e^{-jkr_{n0}}}{r_{n0}} e^{-j2\pi\frac{ln}{N}} \right|^2. \quad (10)$$

This formulation is simpler than (8) for determining the power associated with one OAM mode order.

4. Asymptotic formulation

4.1. Development

The objective of this section is to determine an asymptotic formulation of the link budget (10) at large distances, *i.e.* when $D \rightarrow +\infty$. In other words, we seek the leading term for each value of l . To do so, we firstly rewrite (10) using the standard notation $\langle | \rangle$ for the discrete complex hermitian inner product. This yields

$$\frac{P_{\text{r}}}{P_{\text{t}}}(l) = \left| \frac{\lambda\beta}{4\pi} \left\langle u_n \left| e^{j\frac{2\pi ln}{N}} \right\rangle \right|^2, \quad (11)$$

with $u_n = e^{-jkr_{n0}}/r_{n0}$.

Since r_{n0} is even with n , u_n is even as well. Thus, the previous expression can be written as

$$\begin{aligned} \frac{P_{\text{r}}}{P_{\text{t}}}(l) &= \left| \frac{\lambda\beta}{4\pi} \left\langle u_n \left| \cos\left(\frac{2\pi ln}{N}\right) \right\rangle \right|^2, \\ &= \left| \frac{\lambda\beta}{4\pi} \left\langle u_n \left| \cos\left(\frac{2\pi |l|n}{N}\right) \right\rangle \right|^2. \end{aligned} \quad (12)$$

From this expression, the link budget for the modes $+l$ and $-l$ are the same.

To obtain the asymptotic formulation of $P_{\text{r}}/P_{\text{t}}$, we firstly expand u_n in Taylor series. For r_{n0} , the expression is obtained by writing

$$r_{n0} = D_{\text{tot}} \sqrt{1 - \frac{2R_{\text{t}}R_{\text{r}}}{D_{\text{tot}}^2} \cos\left(\frac{2\pi n}{N}\right)}, \quad (13)$$

with $D_{\text{tot}}^2 = D^2 + R_{\text{t}}^2 + R_{\text{r}}^2$. Thus, an asymptotic expansion of r_{n0} when $D_{\text{tot}} \rightarrow +\infty$ is given by

$$\begin{aligned} r_{n0} &= \sum_{m=0}^{+\infty} \binom{1/2}{m} \frac{(-2R_{\text{r}}R_{\text{t}})^m}{D_{\text{tot}}^{2m-1}} \cos^m\left(\frac{2\pi n}{N}\right) \\ &= D_{\text{tot}} + \sum_{m=1}^{+\infty} \binom{1/2}{m} \frac{(-2R_{\text{r}}R_{\text{t}})^m}{D_{\text{tot}}^{2m-1}} \cos^m\left(\frac{2\pi n}{N}\right), \end{aligned} \quad (14)$$

where $\binom{\alpha}{m}$ are the generalized binomial coefficients. From this result, we deduce

$$e^{-jkr_{n0}} = e^{-jkD_{\text{tot}}} \cdot \exp \left[-jk \sum_{m=1}^{+\infty} \binom{1/2}{m} \frac{(-2R_{\text{r}}R_{\text{t}})^m}{D_{\text{tot}}^{2m-1}} \cos^m \left(\frac{2\pi n}{N} \right) \right]. \quad (15)$$

Similarly, we have

$$\frac{1}{r_{n0}} = \frac{1}{D_{\text{tot}}} \sum_{m'=0}^{+\infty} \binom{-1/2}{m'} \frac{(-2R_{\text{r}}R_{\text{t}})^{m'}}{D_{\text{tot}}^{2m'}} \cos^{m'} \left(\frac{2\pi n}{N} \right). \quad (16)$$

Developing the exponential in (15) and multiplying by (16), we finally obtain

$$u_n = \frac{e^{-jkD_{\text{tot}}}}{D_{\text{tot}}} \sum_{m'=0}^{+\infty} \binom{-1/2}{m'} \frac{(-2R_{\text{r}}R_{\text{t}})^{m'}}{D_{\text{tot}}^{2m'}} \cos^{m'} \left(\frac{2\pi n}{N} \right) \cdot \sum_{q=0}^{+\infty} \frac{(-jk)^q}{q!} \left[\sum_{m=1}^{+\infty} \binom{1/2}{m} \frac{(-2R_{\text{r}}R_{\text{t}})^m}{D_{\text{tot}}^{2m-1}} \cos^m \left(\frac{2\pi n}{N} \right) \right]^q. \quad (17)$$

This expansion is expressed in terms of $\cos^m(2\pi n/N)$ and $\cos^{m'}(2\pi n/N)$ whereas the initial inner product (12) makes use of $\cos(2\pi|l|n/N)$. Nevertheless, from cosine power reduction formulas and from (17), the dominant contribution in $\cos(2\pi|l|n/N)$ is contained in the $\cos^{|l|}(2\pi n/N)$ term. Indeed, lower-order powers of cosine do not contain terms in $\cos(2\pi|l|n/N)$ when linearized, and higher-order terms decrease faster when $D \rightarrow \infty$. Therefore, to obtain the link budget (12) for each mode order l , the dominant component in $\cos^{|l|}(2\pi n/N)$ when $D \rightarrow +\infty$ must be extracted. As a consequence of the limit $D \rightarrow +\infty$, the dominant term is obtained only with the components $m = 1$ and $m' = 0$ in (17), and is given by

$$\frac{e^{-jkD_{\text{tot}}}}{D_{\text{tot}}} \frac{1}{|l|!2^{|l|}} \frac{(jk2R_{\text{r}}R_{\text{t}})^{|l|}}{D_{\text{tot}}^{|l|}} \cos^{|l|} \left(\frac{2\pi n}{N} \right), \quad (18)$$

Adding any other terms in the series only yields components decaying faster.

Finally, from (12) and (18), the link budget is asymptotically given by

$$\begin{aligned} \frac{P_{\text{r}}}{P_{\text{t}}}(|l|) &= \left| \frac{\lambda\beta}{4\pi|l|!} \frac{(kR_{\text{r}}R_{\text{t}})^{|l|}}{D_{\text{tot}}^{|l|+1}} \left\langle \cos^{|l|} \left(\frac{2\pi n}{N} \right) \middle| \cos \left(\frac{2\pi|l|n}{N} \right) \right\rangle \right|^2 \\ &= \left| \frac{\lambda\beta}{4\pi|l|!} \frac{(kR_{\text{r}}R_{\text{t}})^{|l|}}{D_{\text{tot}}^{|l|+1}} \frac{N}{2^{|l|}} \right|^2. \end{aligned} \quad (19)$$

Hence, with $D_{\text{tot}} \simeq D$ when $D \rightarrow +\infty$, the asymptotic OAM single-mode link budget can be expressed as

$$\frac{P_{\text{r}}}{P_{\text{t}}}(|l|) = \left| \frac{\lambda N \beta}{4\pi|l|!} \left(\frac{kR_{\text{t}}R_{\text{r}}}{2} \right)^{|l|} \frac{1}{D^{|l|+1}} \right|^2. \quad (20)$$

This result demonstrates that $P_{\text{r}}/P_{\text{t}}$ decays in $1/D^{2|l|+2}$ for a mode of order $|l|$.

4.2. Validation and convergence

4.2.1. Convergence

In this section we want to study the convergence of the global link budget (10) with the asymptotic formulation (20). In addition, the dependence on the OAM order l is also studied.

The difference between the asymptotic formulation (20) and the non-asymptotic one (10) can be estimated. For any distance, we can compute the relative difference given by

$$\mathcal{E} = \frac{|P_{\text{r}}/P_{\text{t}} - (P_{\text{r}}/P_{\text{t}})_{\text{asympt}}|}{|P_{\text{r}}/P_{\text{t}}|}. \quad (21)$$

From the results in Fig. 4, the distances at which the relative difference levels are at least of 1% depend on l but the farthest distance is given by the OAM mode order $l = 0$. Therefore the traditional method to determine the far field distance remains

the same and can be applied for every OAM mode order and are conventionally dependent on the radii. Thus, in the far field, the asymptotic formulation (20) holds.

4.2.2. Asymptotic slope

In order to study the formulation (20), we show in Fig. 5 the link budgets from (10) and (20) computed for $|l| = 0, 1, 2, 3, 4$ and $R_t = R_r = 5\lambda$. As expected, the two representations converge. From the Fraunhofer distance $2(2 \max(R_t, R_r))^2/\lambda = 200\lambda$, the link budget asymptotically tends to straight lines of slope $-20(|l| + 1)$ dB/decade, which is consistent with an attenuation in $1/D^{2|l|+2}$. This was first discovered in *Tamagnone et al.* [2012] for the case $l = 1$ with a two element antenna array system, and extended for all the OAM mode orders in *Tamagnone et al.* [2013] with the Laguerre-Gaussian beam formalism. Here we confirm this result and extend it for any circular array antenna system. This result highlights the strong asymptotic slope for non-zero OAM mode orders. This will be discussed in the following sections and in the conclusion.

Finally, with this expression (20), we can calculate immediately the link budget. In addition, we have validated the decay in $1/D^{2|l|+2}$ of waves carrying OAM. In the next section we study the asymptotic formulation of the link budget (20) in terms of gains and losses.

5. Gain and free-space losses

5.1. Asymptotic Expressions

In this section, we generalise the classical transmission equation (1) to non-zero OAM mode order. To do so, we define equivalent antenna gains G_{teq} , G_{req} and equivalent losses L_{FSeq} . They depend on the characteristics of the antennas, on the distance and on the OAM order l .

Keeping in mind $L_{\text{FS}} = (4\pi D/\lambda)^2$, we want to find a formulation with only gains and losses, *i.e.*

$$\frac{P_{\text{r}}}{P_{\text{t}}}(l) = G_{\text{teq}}(l) G_{\text{req}}(l) \frac{1}{L_{\text{FSeq}}(l)}. \quad (22)$$

With some transformations in (20), we can obtain

$$\frac{P_{\text{r}}}{P_{\text{t}}}(l) = \frac{Ng_{\text{t}}}{|l|!} \left(\frac{4\pi(\pi R_{\text{t}}^2)}{\lambda^2} \right)^{|l|} \frac{Ng_{\text{r}}}{|l|!} \left(\frac{4\pi(\pi R_{\text{r}}^2)}{\lambda^2} \right)^{|l|} \left(\frac{\lambda}{4\pi D} \right)^{2|l|+2}. \quad (23)$$

In this equation, we can identify equivalent free-space losses

$$L_{\text{FSeq}}(l) = \left(\frac{4\pi D}{\lambda} \right)^{2|l|+2}. \quad (24)$$

Note that the free-space losses have exactly the classical expression $L_{\text{FS}} = (4\pi D/\lambda)^2$ but with an exponent $|l| + 1$, which gives $L_{\text{FSeq}}(l) = (L_{\text{FS}})^{|l|+1}$.

From (22) and (23), we also define equivalent OAM antenna gains for a configuration with two face-to-face circular array antennas. Their expressions are given by

$$G_{\text{eq}}(l) = \frac{Ng}{|l|!} \left(\frac{4\pi(\pi R^2)}{\lambda^2} \right)^{|l|}. \quad (25)$$

Since from the beginning we have separated the transmitter and receiver parts, the formulation (23) remains valid for a communication system with two different array antenna radii. In addition, this formula is only valid for array antennas.

5.2. Equivalent array antenna gain study

The equivalent gain (25) is dependent on the antenna parameters. When $l = 0$, we have $G_{\text{teq}} = G_{\text{req}} = Ng$ which is classical for an array antenna with elements fed in-phase with neglected couplings. When $l \neq 0$, G_{teq} and G_{req} are dependent on N , R_t , R_r and l . Therefore, the transmitted and received equivalent gains can be modified to partially compensate the free-space losses in $1/D^{2|l|+2}$ at a given distance. In Fig. 6, equation (23) of the link budget is computed for a transmission between two circular array antennas separated by a distance of $D = 1000\lambda$ where $R = R_t = R_r$ varying from 1λ to 10λ . A comparison with (10) is also plotted to confirm the asymptotic behaviour. For a fixed value of $|l|$, each equivalent gain increases in $R^{2|l|}$ so that the link budget improves by a factor of $R^{4|l|}$. On the contrary, for a fixed value of R , when $|l|$ increases, the link budget decreases since asymptotically the effect of D is greater than those of R_t and R_r .

6. Simulation

A general asymptotic formulation (23) of the link budget has been obtained and validated. It matches the classical theory (1) and can give the OAM single-mode link budget. In this section, another validation with the commercial electromagnetic simulation software Feko is performed.

6.1. Setup

The same system as before with two identical face-to-face array antennas is modelled in the software. We choose to have 8 elements per array. This will allow the generation of the OAM mode orders $|l| = 0, 1, 2$.

6.1.1. Array antenna element

For the array elements, we use rectangular patch antennas designed to work at 2.42GHz, as depicted in Fig. 7. For the sake of simplicity, the dielectric substrate is air and the patch is fed by a wire source between the patch and the ground plane in such a way that a linear polarisation is excited. In the simulation results, the antenna gain of the element is 8.70dBi. This value is given to the terms g_t and g_r in the asymptotic formulation (23).

6.1.2. Array antenna

The 8 element array and its radiation patterns for OAM mode orders $|l| = 0, 1, 2$ are represented in Fig. 8. There are many grating lobes caused by the annular geometry of the array. However, along the array axis, a good OAM radiation pattern is generated and is convenient for the simulation.

The far field is here obtained beyond the Fraunhofer distance located at 200λ for the arrays of radii 5λ . The simulations are performed with two face to face arrays using the same polarisation.

The S-parameters between each port of the arrays are computed to obtain the simulated propagation channel matrix so that all the couplings are directly included in the S-parameter. The BFN is still considered as ideal. So the matrix equation

(7) can be used to calculate all the link budgets but now with simulated values for \mathbf{H}_{tot} , taking mutual couplings into account.

6.2. Parametric Simulations

6.2.1. Distance

First, we want to verify the asymptotic slope in $1/D^{2|l|+2}$. A parametric study is performed on the distance between the two array antennas and the results are displayed in Fig. 9. The results show a good match and Fig. 9 clearly shows the slope in $1/D^{2|l|+2}$ beyond the Fraunhofer distance of 200λ .

6.2.2. Radii

The antenna gain behaviour with respect to the array radii, highlighted in section 5.2, is verified in the simulation depicted in Fig. 10. The results show a good match and illustrate the usefulness of changing the array radii to optimise the link budget.

6.3. Conclusion on the Simulations

In this section, we have compared the simulated link budget with the asymptotic formulation (23). The results show a very good match and validate the formulations of Section 4.

Finally, for circular arrays, the asymptotic formulation (23) allows to calculate the link budget of an OAM system instantly. As for the classical Friis transmission equation, the asymptotic formulation (23) can be very useful in a OAM system pre-design and clearly shows the impact of each parameter of the system on the link

budget. The good match in the results confirms that the common hypotheses taken beforehand, like neglecting couplings, can be consistent in these conditions.

For non-zero OAM mode, the high asymptotic slope due to the free space losses is determining in the system design. A trade-off with the antenna gains can be achieved to reach the requirement. However, as shown in *Edfors and Johansson* [2012], in the very far field, the higher order OAM waves become rapidly weak and only the $l = 0$ OAM mode remains usable.

7. Conclusion

We have presented an original formulation of the link budget with equivalent OAM gains and free-space losses dependent on the OAM order l . For an OAM system design, it clearly shows the impact of each system parameter on the link budget.

In this paper, we have investigated the asymptotic formulation of the OAM link budget. From the classical theory we have seen that the OAM link budget cannot be calculated as usual. We have also studied a configuration with two circular array antennas. This system is simple but sufficient enough to study the general properties of the OAM. We have found an asymptotic formulation of the link budget by means of asymptotic expansions. An asymptotic decay in $1/D^{2|l|+2}$ has been observed. The calculation have shown that the asymptotic formulation holds from a distance which classically depend on the OAM mode order $l = 0$. The equivalent gain formula has been studied and highlights the influence of R , l and of the array elements on the link budget. Finally, the calculated formulations have been validated with the results

of the commercial electromagnetic simulation software Feko. This clearly shows the advantage of our formulas for a rapid system design.

The study has shown some elements on the link budget for the use of the new degree of freedom offered by the OAM in the case of superimposition of several channels on the same bandwidth. The proposed formulation is specific to face-to-face circular arrays but the theory may be extended to generalize this formulation to other configurations, *e.g.* a continuous aperture.

Nonetheless, the results that we have shown confirm the difficulties to use OAM at very large distance. However, at shorter distances, they remain of interest because there exists communication configurations in which the link budget is more suitable.

Acknowledgments. We thank Direction Générale de l'Armement (DGA) and Centre National d'Etudes Spatiales (CNES) for their financial support to this work.

References

- Allen, L., M. W. Beijersbergen, R. J. C. Spreeuw, and J. P. Woerdman (1992), Orbital angular momentum of light and the transformation of laguerre-gaussian laser modes, *Phys. Rev. A*, *45*, 8185–8189, doi:10.1103/PhysRevA.45.8185.
- Bai, Q., A. Tennant, and B. Allen (2014), Experimental circular phased array for generating oam radio beams, *Electronics Letters*, *50*(20), 1414–1415, doi: 10.1049/el.2014.2860.
- Beijersbergen, M., R. Coerwinkel, M. Kristensen, and J. Woerdman (1994), Helical-wavefront laser beams produced with a spiral phaseplate, *Optics Communications*,

112(56), 321 – 327, doi:[http://dx.doi.org/10.1016/0030-4018\(94\)90638-6](http://dx.doi.org/10.1016/0030-4018(94)90638-6).

Bennis, A., R. Niemiec, C. Brousseau, K. Mahdjoubi, and O. Emile (2013), Flat plate for oam generation in the millimeter band, in *Antennas and Propagation (EuCAP), 2013 7th European Conference on*, pp. 3203–3207.

Beth, R. A. (1936), Mechanical detection and measurement of the angular momentum of light, *Phys. Rev.*, 50, 115–125, doi:10.1103/PhysRev.50.115.

Chan, R. H.-F., and X.-Q. Jin (2007), *An Introduction to Iterative Toeplitz Solvers*, Fundamentals of Algorithms, Society for Industrial and Applied Mathematics, Philadelphia, PA.

Diallo, C., D. K. Nguyen, A. Chabory, and N. Capet (2014), Estimation of the orbital angular momentum order using a vector antenna in the presence of noise, in *Antennas and Propagation (EuCAP), 2014 8th European Conference on*, pp. 3858–3862.

Djordjevic, I. (2011), Ldpc-coded oam modulation and multiplexing for deep-space and near-earth optical communications, in *Space Optical Systems and Applications (ICSOS), 2011 International Conference on*, pp. 325–333, doi:10.1109/ICSOS.2011.5783692.

Edfors, O., and A. Johansson (2012), Is orbital angular momentum (oam) based radio communication an unexploited area?, *Antennas and Propagation, IEEE Transactions on*, 60(2), 1126–1131, doi:10.1109/TAP.2011.2173142.

Gibson, G., J. Courtial, M. Padgett, M. Vasnetsov, V. Pas'ko, S. Barnett, and S. Franke-Arnold (2004), Free-space information transfer using light beams

- carrying orbital angular momentum, *Opt. Express*, *12*(22), 5448–5456, doi:10.1364/OPEX.12.005448.
- Jackson, J. D. (1999), *Classical electrodynamics*, 3rd ed. ed., Wiley, New York, NY.
- Krenn, M., R. Fickler, M. Fink, J. Handsteiner, M. Malik, T. Scheidl, R. Ursin, and A. Zeilinger (2014), Communication with spatially modulated light through turbulent air across vienna, *New Journal of Physics*, *16*(11), 113,028.
- Mohammadi, S., L. Daldorff, J. Bergman, R. Karlsson, B. Thidé, K. Forozesh, T. Carozzi, and B. Isham (2010), Orbital angular momentum in radio - a system study, *Antennas and Propagation, IEEE Transactions on*, *58*(2), 565–572, doi:10.1109/TAP.2009.2037701.
- Nguyen, D. K., O. Pascal, J. Sokoloff, A. Chabory, B. Palacin, and N. Capet (2014), Discussion about the link budget for electromagnetic wave with orbital angular momentum, in *Antennas and Propagation (EuCAP), 2014 8th European Conference on*, pp. 1311–1315.
- Niemiec, R., C. Brousseau, O. Emile, and K. Mahdjoubi (2012), Transfer of orbital angular momentum on a macroscopic object in the uhf frequency band, *AES2012 - Advanced Electromagnetics Symposium*.
- Padgett, M., and L. Allen (1995), The poynting vector in laguerre-gaussian laser modes, *Optics Communications*, *121*(13), 36 – 40, doi:[http://dx.doi.org/10.1016/0030-4018\(95\)00455-H](http://dx.doi.org/10.1016/0030-4018(95)00455-H).
- Poynting, J. H. (1909), The wave motion of a revolving shaft, and a suggestion as to the angular momentum in a beam of circularly polarised light, *Proceedings of*

the Royal Society of London A: Mathematical, Physical and Engineering Sciences, 82(557), 560–567, doi:10.1098/rspa.1909.0060.

Soskin, M. S., V. N. Gorshkov, M. V. Vasnetsov, J. T. Malos, and N. R. Heckenberg (1997), Topological charge and angular momentum of light beams carrying optical vortices, *Phys. Rev. A*, 56, 4064–4075, doi:10.1103/PhysRevA.56.4064.

Tamagnone, M., C. Craeye, and J. Perruisseau-Carrier (2012), Comment on 'encoding many channels on the same frequency through radio vorticity: first experimental test', *New Journal of Physics*, 14(11), 118,001.

Tamagnone, M., C. Craeye, and J. Perruisseau-Carrier (2013), Comment on 'reply to comment on "encoding many channels on the same frequency through radio vorticity: first experimental test"', *New Journal of Physics*, 15(7), 078,001.

Tamburini, F., E. Mari, A. Sponselli, B. Thidé, A. Bianchini, and F. Romanato (2012a), Encoding many channels on the same frequency through radio vorticity: first experimental test, *New Journal of Physics*, 14(3), 033,001.

Tamburini, F., B. Thidé, E. Mari, A. Sponselli, A. Bianchini, and F. Romanato (2012b), Reply to comment on 'encoding many channels on the same frequency through radio vorticity: first experimental test', *New Journal of Physics*, 14(11), 118,002.

Tamburini, F., E. Mari, G. Parisi, F. Spinello, M. Oldoni, R. A. Ravanelli, P. Coassini, C. G. Someda, B. Thid, and F. Romanato (2015), Tripling the capacity of a point-topoint radio link by using electromagnetic vortices, *Radio Science*.

- Thidé, B., H. Then, J. Sjöholm, K. Palmer, J. Bergman, T. D. Carozzi, Y. N. Istomin, N. H. Ibragimov, and R. Khamitova (2007), Utilization of photon orbital angular momentum in the low-frequency radio domain, *Phys. Rev. Lett.*, *99*, 087,701, doi: 10.1103/PhysRevLett.99.087701.
- Torres, J. P., and L. Torner (2011), *Twisted Photons: Applications of Light with Orbital Angular Momentum*, Wiley.

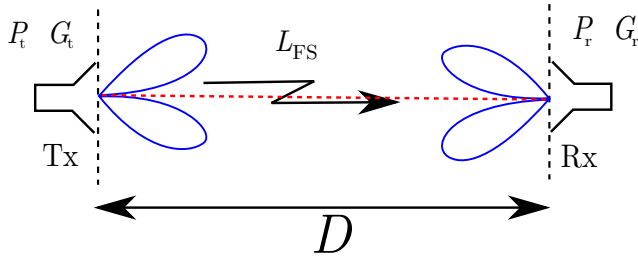


Figure 1. Standard configuration for the transmission of waves with non-zero OAM in a single mode configuration. (radiation patterns in blue)

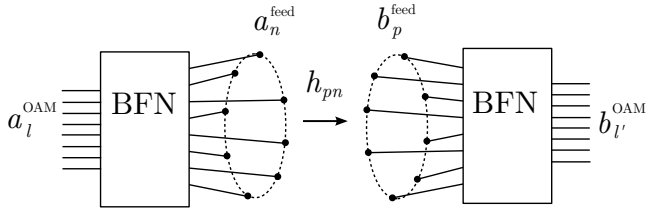


Figure 2. Main elements for an OAM transmission with circular arrays.

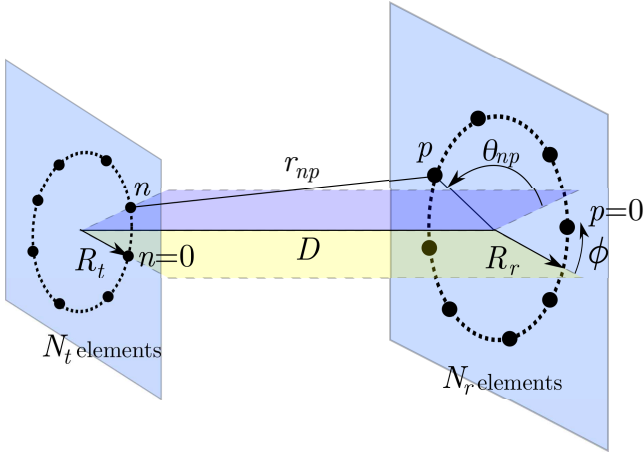


Figure 3. Geometry of the circular arrays where the position of each antenna element is equidistant along the perimeters of the circular arrays.

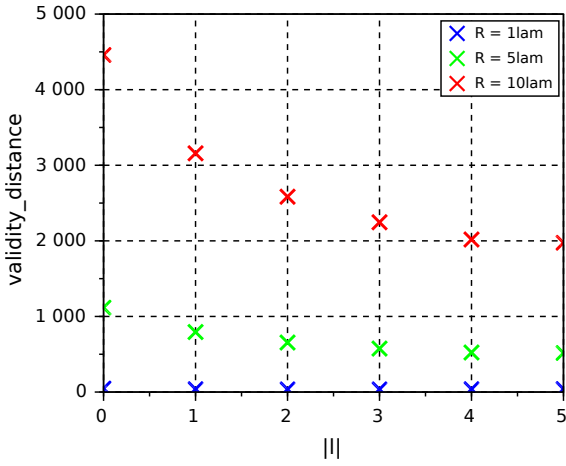


Figure 4. Distance from which 1% relative difference level is reached with $N = 12$ and for different values of $R = R_t = R_r$.

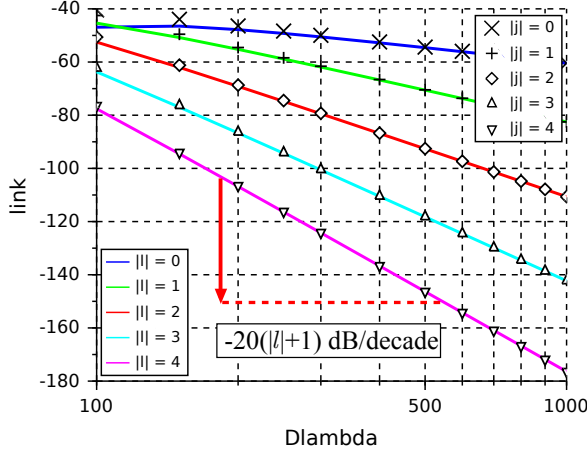


Figure 5. Link budgets for $|l| = 0, 1, 2, 3, 4$ with $N = 12$, $R = R_t = R_r = 5\lambda$ and $g_t = g_r = 1$. The link budget (10) is depicted in color lines, and the asymptotic formulation (20) is represented with dots.

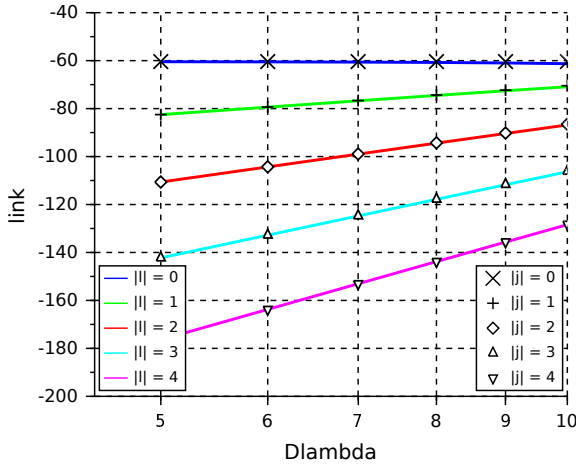


Figure 6. Link budgets for $|l| = 0, 1, 2, 3, 4$ with $N = 12$, $R = R_t = R_r$, $g_t = g_r = 1$ and $D = 1000\lambda$. The link budget (10) is depicted in color lines, and the asymptotic formulation (20) is represented with dots.

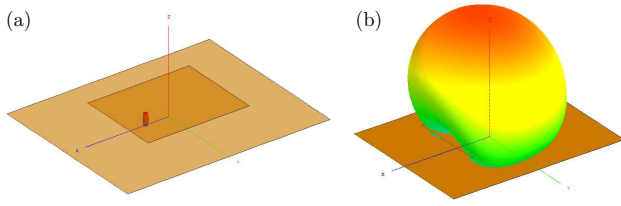


Figure 7. (a) 3D model of a single rectangular patch designed for 2.42GHz and only one linear polarisation. (b) Its radiation pattern.

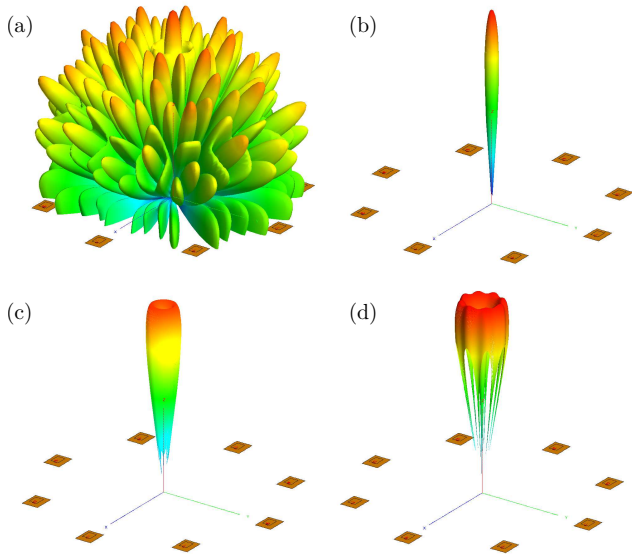


Figure 8. (a) Radiation patterns of the circular array for the OAM mode order $l = 0$. Due to the high grating lobes (b) (c) (d) show the radiation patterns for the OAM mode orders $|l| = 0, 1, 2$ in the vicinity of the array axis.

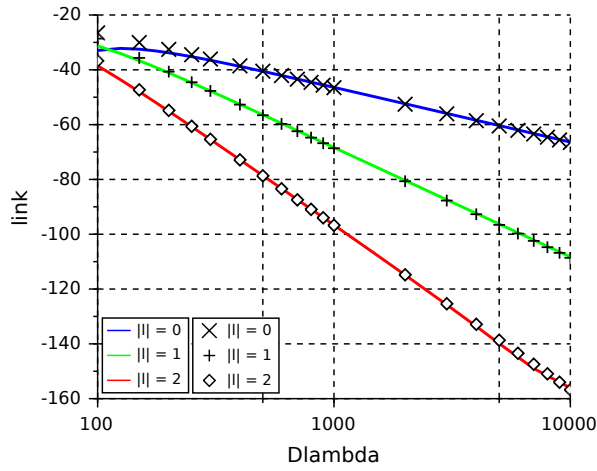


Figure 9. Simulated link budget between the two array antennas of radii 5λ in function of the distance D . The simulated link budget is depicted in color lines, and the calculated link budget with the asymptotic formulation (23) is represented with dots.

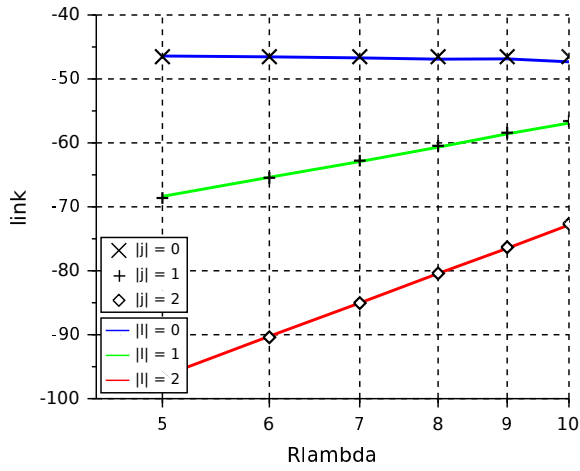


Figure 10. Simulated link budget between both array antennas separated by 1000λ in function of the array radii. The simulated link budget is depicted in color lines, and the calculated link budget with the asymptotic formulation (23) is represented with dots.